



# Spectroscopic features of radiolytic intermediates induced in gamma irradiated sulfatiazole: an ESR study

Şeyda Çolak, Mustafa Korkmaz\*

*Physics Engineering Department, Hacettepe University, 06800 Beytepe, Ankara, Turkey*

Received 22 September 2003; received in revised form 11 June 2004; accepted 17 June 2004

Available online 15 September 2004

## Abstract

Sulfonamides are used as active ingredients in different drugs to treat infections caused by bacteria. Sulfatiazole (STZ) is one of the commonly used sulfonamides as antibacterial agent in drugs, which constitute potential candidates for radiosterilization. However, the crucial point in this respect is to monitor the amount and characteristic features of the radiolytic intermediates produced after irradiation. Electron spin resonance (ESR) spectroscopy is extensively used for this purpose due to its high sensitivity toward intermediates exhibiting radicalic nature. Thus, the aim of the present work is to investigate the spectroscopic and kinetic features of the species having unpaired electrons induced in gamma irradiated STZ at room and different temperatures in the dose range of 5–50 kGy using ESR spectroscopy. Spectra of irradiated STZ consisted of many resonance peaks in the studied dose and temperature ranges. Heights of the peaks measured with respect to the base line were used to monitor microwave, temperature, time-dependent features of the radical species contributing to the experimental ESR spectra. Four tentative species of different spectroscopic and structural features assigned as A, B, C and D were found well explaining the experimental ESR spectra of gamma irradiated STZ. Comparison between the principal IR bands of unirradiated and gamma irradiated samples showed no detectable changes and appearance of new bands.

© 2004 Elsevier B.V. All rights reserved.

*Keywords:* Radiosterilization; Sulfonamides; Sulfatiazole; Radical kinetics; ESR

## 1. Introduction

Gamma radiation has emerged as a useful, efficient and economic tool for sterilization of many drugs in their final containers, and it is more actively used now

than at any time (Gopal, 1978; Bhalla et al., 1983; Jacobs, 1995; Reid, 1995). The advantages of sterilization by irradiation include high penetrating power, low chemical reactivity, low measurable residues, small temperature rise and the fact that there are fewer variables to control (Basly et al., 1996; Barbarin et al., 1999; Gibella et al., 2000). However, the adoption of this method requires detailed investigations to ensure that no undesirable changes take place, as ionizing

\* Corresponding author. Tel.: +90 312 2977213;  
fax: +90 312 2992037.

E-mail address: [seyda@hacettepe.edu.tr](mailto:seyda@hacettepe.edu.tr) (M. Korkmaz).

radiation has been reported to cause degradation in the pharmaceuticals and therefore, creating reactive molecular fragments (Miyazaki et al., 1994; Schuler, 1994; Boess and Bögl, 1996), which may result in a toxicological hazard.

Electron spin resonance (ESR) technique appears to be well suited for determination of low concentration of free radicals in complex media and could permit the elucidation of mechanism of radiolysis even for a small radiation dose. Moreover, other features such as high sensitivity, precision, ease and non-destructive read-out make ESR superior to other proposed analytical techniques (Onori et al., 1996) to study radiolytic intermediates produced in irradiated solid samples. Previous results have already shown the suitability of ESR for the detection of irradiated drugs and foods (Bögl, 1989; Delincée, 1991; Desrosiers et al., 1991; Raffi et al., 1992, 1994; Ciranni Signoretto et al., 1993, 1994; Miyazaki et al., 1994; Raffi, 1998; Basly et al., 1999).

Although STZ is used in the sulfonamide containing drugs at a large extent, the applicability of the sterilization by radiation to the solid drugs containing STZ is not yet investigated in the literature. Therefore, the aims of the present work are: to characterize the radiolytic intermediates carrying unpaired electrons produced in gamma irradiated STZ in the dose range of 5–50 kGy and to explore the potential contribution of ESR technique in investigating the radiosterilization of STZ and/or drug delivery system containing STZ as active ingredient, through a detailed ESR study.

## 2. Materials and methods

Sulfatiazole or with its chemical name, 4-amino-*N*-(thiazol-2-yl)benzenesulfonamide of spectroscopic grade was provided from Faculty of Pharmacy of Hacettepe University (Ankara) and was stored at room temperature in a well-closed container protected from light. No further purification was performed, and it was used as it was received. STZ is a white crystalline powder, which slowly darkens on exposure to light. The melting point of prismatic rods is about 200–204 °C while the other phase forms, six-sided plates and prisms, melt about 175 °C or invert, at a lower temperature, to the high-melting phase (Clarke's Isolation and Identification of Drugs in Pharmaceutics, 1986; The Merck Index, 1989). It has a molecular structure

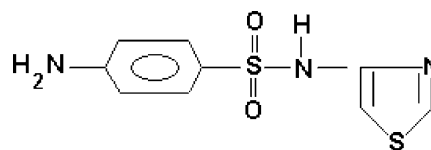


Fig. 1. Molecular structure of sulfatiazole.

given in Fig. 1. Irradiations were performed at room temperature using a <sup>60</sup>Co gamma cell supplying a dose rate of 2.52 kGy/h as an ionizing radiation source at the Sarayköy Establishment of Turkish Atomic Energy Agency in Ankara. The dose rate at the sample sites was measured by a Fricke dosimeter. Investigations were performed on samples irradiated at four different doses (5, 10, 25 and 50 kGy).

ESR measurements were carried out using Varian 9'-E line-X band ESR spectrometer operating at 9.5 GHz and equipped with a TE<sub>104</sub> rectangular double cavity containing a standard sample (DPPH) in the rear resonator which remained untouched throughout the experiment. Signal intensities were calculated from first derivative spectra and compared with that obtained for a standard sample (DPPH) under the same spectrometer operating conditions. Sample temperature inside the microwave cavity was monitored with a digital temperature control system (Bruker ER 4111-VT). The latter provided the opportunity of measuring the temperature with an accuracy of 0.5 K at the site of the sample. A cooling, heating and subsequent cooling cycle was adopted to monitor the evolution of the ESR line shape with temperature using samples irradiated at room temperature. The latter was first decreased to 110 K starting from room temperature, then increased to 402 K with an increment of 20 K and finally was decreased again to room temperature. Variations in the line shape and in the signal intensities with microwave power were also studied in the range 1–80 mW for samples irradiated at room temperature.

Kinetic studies of the contributing free radicals were performed at different temperatures. To achieve this goal, the samples irradiated at room temperature were heated to predetermined temperatures (310, 348, 365, 393 and 413 K) kept at these temperatures for predetermined times (3, 5, 10, 11, 15, 20, 30, 40, 45, 55, 65, 75, 80, 95, 120, 140 and 200 min); then, they were cooled to room temperature and their ESR spectra were recorded. The results were the average of five replicates

for each radiation dose. A simulation calculation based on a model of four tentative radical species, anticipating from the results of microwave saturation and annealing studies, was performed to determine the spectroscopic features of the contributing free radicals.

IR spectra of unirradiated and 50 kGy gamma-irradiated STZ samples were also recorded using Nicolet 520 FT-IR spectrometer and a comparison between the principal IR bands of STZ molecule was performed to monitor the radiolytic products silent to ESR spectroscopy.

### 3. Experimental results and discussion

#### 3.1. General features of the ESR spectra

Although unirradiated STZ exhibited no ESR signal, samples irradiated at room temperature showed a complex ESR spectrum consisting of 10 resonance peaks. Room temperature spectra recorded for two samples irradiated at two different radiation doses are given in Fig. 2a and b with the assigned peak numbers. The most intense resonance line appearing in the

middle of the spectrum was found to have a  $g$  value of 2.0045 and a peak to peak width of 5.2 G. Increase in the absorbed dose caused more intense spectra without creating change in pattern. Thus, it was concluded that irradiation dose was not an important parameter in the formation of the shape of the ESR spectrum of STZ.

Variations of the heights, which were measured with respect to spectrum base line and normalized to the receiver gain, the mass of the sample and the intensity of the standard of these resonance peaks with applied microwave power in the range of 1–80 mW were studied first. The results of these studies indicate that heights of the assigned peak saturate with different rates as inhomogeneously broadened resonance lines do. Microwave saturation behaviours of the studied resonance peaks and the results of spectrum simulation calculations conducted us to propose four different radical species of different characteristics, to explain experimental results obtained in the present work. Therefore, a theoretical function (Eq. (1)) obtained by the sum of four different exponentially growing functions associated with the contributing radical species and best fitting to microwave saturation data derived from room temperature spectra was tried (Stark, 1970)

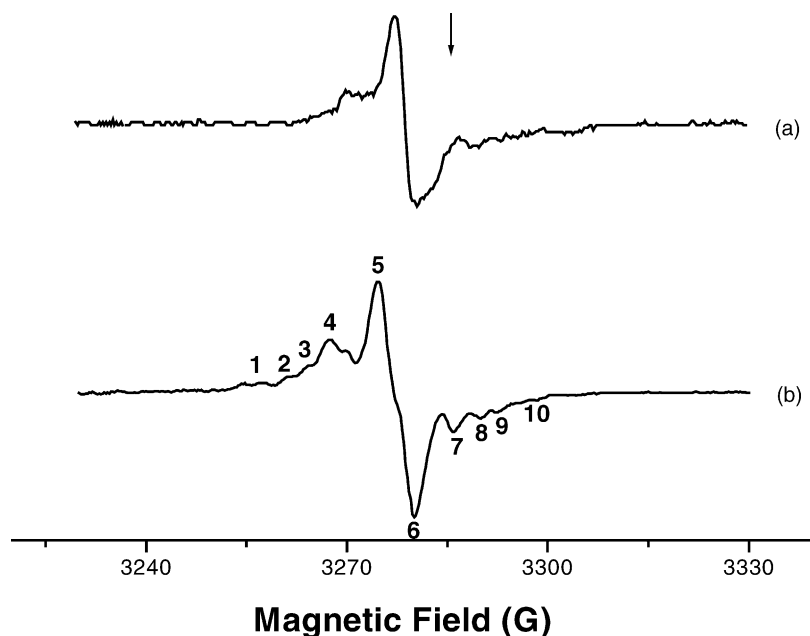


Fig. 2. Room temperature ESR spectra of STZ irradiated at two different doses (a) 5 kGy, (b) 50 kGy. Arrow indicates the position of DPPH line.

Table 1  
Characteristic parameters calculated from microwave saturation data for contributing radical species

Radical species	Parameters		Correlation coefficient ( $r^2$ )
	$d$ (mW) $^{-1}$	$I_0$ (a.u.)	
A	0.350 ( $\pm 0.040$ )	0.06	0.98
B	0.031 ( $\pm 0.003$ )	0.21	
C	0.870 ( $\pm 0.010$ )	0.01	
D	0.160 ( $\pm 0.050$ )	0.73	

Figures in parenthesis represent the estimated error on the relevant parameters.

to elucidate experimental microwave saturation data.

$$I = I_{A0}(1 - e^{-d_A \times P}) + I_{B0}(1 - e^{-d_B \times P}) + I_{C0}(1 - e^{-d_C \times P}) + I_{D0}(1 - e^{-d_D \times P}) \quad (1)$$

In Eq. (1),  $P$  is the microwave power in mW;  $I_{0s}$  and  $d_s$  stand for intensities at saturation and growth parameters related with the involved radical species assigned as A, B, C and D, respectively. Characteristic parameters calculated by this technique for contributing species are summarized in Table 1.

### 3.2. Dose–response curves

A higher concentration of radicals generated at the same absorbed dose of radiation, indicates a higher sensitivity of the substance toward the type of radiation used. Radiation sensitivity of STZ was also studied through the variations of the peak heights with absorbed gamma radiation dose (Fig. 3). They are found to follow a function of the type given in Eq. (2) with different growth rate parameter in the studied dose range (0–50 kGy)

$$I = I_0(1 - e^{-b \times D}) \quad (2)$$

In Eq. (2),  $D$  and  $b$  stand for absorbed dose in kGy and radiation dose growth parameters, respectively and  $I_0$  represents peak height at saturation. Parameter values calculated by fitting (Stark, 1970) experimental dose–response data obtained for each peak to Eq. (2) are summarized in Table 2. As seen from this table, the radiation dose growth parameter  $b$  of the studied peaks are different. This means, once more, that more than one radical species contribute to the formation of each resonance peaks.

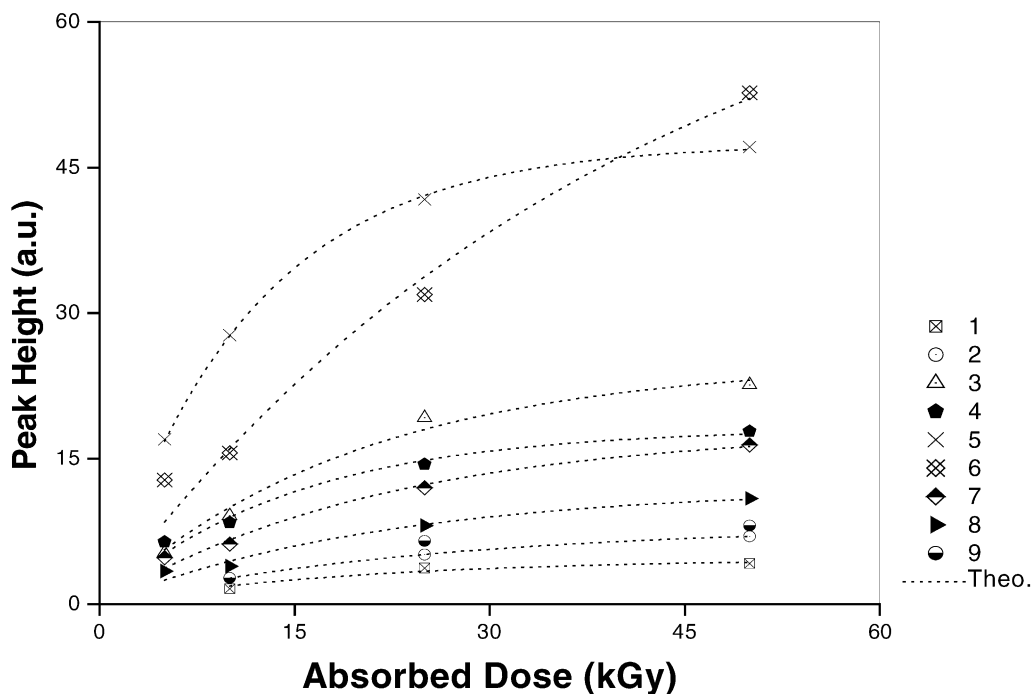


Fig. 3. Variations of peak heights with absorbed radiation dose. Dashed lines represent theoretical curves best fitting to experimental data.

Table 2  
Parameters best describing experimental dose–response data of studied resonance peaks

Peak	Parameter		Correlation coefficient ( $r^2$ )
	$I_0$ (a.u.)	$b$ (kGy) $^{-1}$	
1	4.7	0.052	0.95
2	8.1	0.040	0.99
3	25.1	0.051	0.99
4	18.1	0.068	0.98
5	47.6	0.087	0.99
6	73.9	0.024	0.98
7	18.1	0.046	0.98
8	12.1	0.046	0.97
9	9.5	0.040	0.97

### 3.3. Stabilities of the radical species at normal and stability conditions

Stabilities of the radiolytic intermediates in an irradiated drug or drug raw material are also important. Therefore, this feature of the radicals produced in irradiated STZ was also studied. Samples irradiated at different radiation doses were used to achieve this goal.

The decay of the peak heights of the samples irradiated at different doses and stored in well-closed container at normal (290 K) and stability conditions (313 K and 75% relative humidity) were found to be independent from the irradiation dose. Thus, the peak height decay data, obtained for a sample irradiated at a dose of 50 kGy, were used to get the decay characteristics of the contributing radicals under both storing conditions. The data relative to the decay of some characteristic peaks are given in Fig. 4. The decays over a period of 90 days of the peak heights of the samples stored at normal conditions were calculated best fitting (Stark, 1970) to the sum of four exponentially decaying functions of different weights and of different decay constants as given in Eq. (3).

$$I = I_{A0}e^{-k_A t} + I_{B0}e^{-k_B t} + I_{C0}e^{-k_C t} + I_{D0}e^{-k_D t} \quad (3)$$

In the last equation,  $t$ ,  $I_{0s}$ , and  $k_s$  stand for the time elapsed after stopping irradiation, the initial signal intensities and decay constants, respectively, for contributing radical species. This result which agrees with the microwave saturation data, was considered, once more, as the justification of the presence of more than

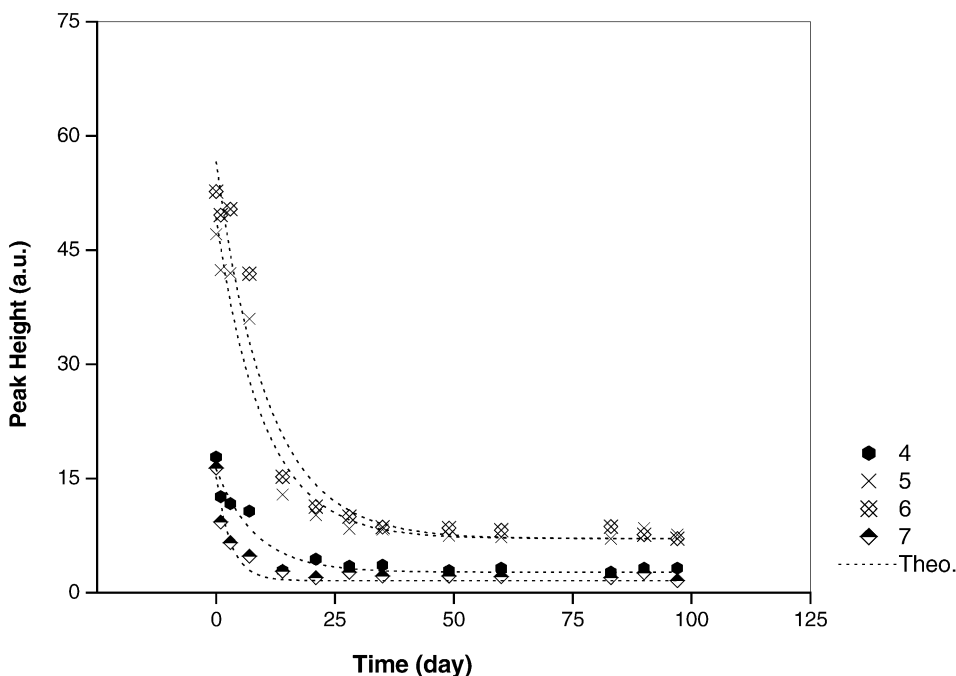


Fig. 4. Variations of the characteristic peak heights with time at normal conditions.

Table 3  
Decay constants for the contributing radicals calculated from normal conditions long term peak height decay data

Irradiation dose (kGy)	Radical species	Decay constants $k \times 10^5$ (day) <sup>-1</sup>	Correlation coefficient ( $r^2$ )
50	A	1483 ( $\pm 107$ )	0.98
	B	8400 ( $\pm 420$ )	
	C	1178 ( $\pm 95$ )	
	D	9800 ( $\pm 450$ )	

Figures in parenthesis indicate the estimated error on the relevant parameters.

one radical species of different decay characteristics contributing to the formation of the ESR spectra of irradiated STZ. The data derived from the decay of the signal intensities at normal conditions are summarized in Table 3. Contributing radicals were calculated to decay much faster at stability conditions (313 K and 75% relative humidity). The decay results relative to the stability condition studies are not given here to save space.

### 3.4. Variations of peak heights with temperature

A variable temperature study relative to the variations of the peak heights with temperature in the ranges of 293–110 and 292–402 K was also performed. Cooling the sample down to room temperature caused slight reversible increases and/or decreases in the resonance peak heights likely due to the presence in irradiated samples of radical species of different microwave saturation behaviours at low temperature. Namely, below room temperature, variation in a given resonance peak height is determined, in large extent, by the saturation characteristics of most significantly contributing radical or radicals. This variation can be a decrease or an increase depending whether it (they) was (were) saturated or not at low temperature. Warming the sample above room temperature produced practically no changes in the heights of all observed peaks up to 320 K. However, increase of the sample temperature above 320 K caused continuous decreases in the heights of all resonance peaks. Relatively sharp decreases, especially in the heights of 5th and 6th peaks, were observed to occur. Above 372 K, ESR spectrum of STZ turned out into a singlet resonance line. This indicates that at high temperatures, most of the radical species were decayed completely except that or those contributing to the cen-

tral line ( $g = 2.0045$ ). The decreases at high temperatures in all peak heights were irreversible due to relatively high decays of the contributing radical species at these temperatures. This result incited us to perform annealing studies on irradiated STZ to determine the decay constant at high temperatures and thus, to calculate the activation energies relevant to the radical decay processes.

### 3.5. Radical decays in annealed samples

Radical decay rates depend on the nature of the matrix containing radicals, and annealing is a constant process with local diffusion of radicals and molecules in some softening of defects or irregularities (Tilquin, 1985). Radical species responsible for ESR spectrum of irradiated STZ are expected to have different decay characteristics depending on the sample temperature. In other terms, the decay rates of the radicals at high temperature are expected to be higher than the decay rates at low temperatures. In fact, it was found that it was the case. Increase in temperature accelerated the decays of the radicals and the higher the temperature, the higher were the decay rates. The decay results relative to the height of peak 5 of a sample irradiated at a dose of 50 kGy and annealed at different temperatures for different times are given Fig. 5 as an example of these variations. Similar decay graphs were obtained for other resonance peaks, but they were not given here to save space. Experimental peak height decay data obtained for samples annealed at different temperatures were used to calculate the decay constants of the contributing radicals at the annealing temperatures assuming that radicals follow a first-order kinetics as given by Eq. (3). A model of four radical species of different decay constants decaying with assumed kinetics were found to fit best the experimental signal intensity decay data. Dotted lines in Fig. 5, which are derived through a curve-fitting method (Stark, 1970) show the theoretical curves obtained by this procedure. Decay constants calculated for radicals contributing to the formation of the ESR spectra of the STZ samples irradiated at a dose of 50 kGy and annealed at five different temperatures are summarized in Table 4. An Arrhenius plot was also constructed to determine the activation energies of the contributing radical species, and the values given in Table 5 were obtained.

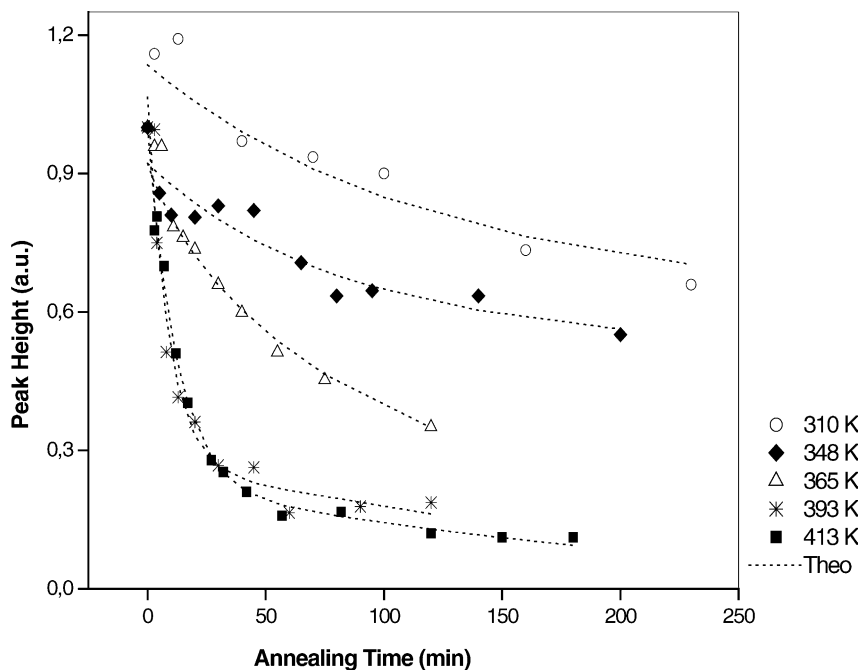


Fig. 5. High-temperature decay results for peak 5 of a sample irradiated at a dose of 50 kGy and annealed at five different temperatures ((○) (310 K), (◆) (348 K), (△) (365 K), (※) (393 K), (■) (413 K)) for different times.

### 3.6. Proposed radical species and spectra simulations

SO<sub>2</sub> is the most sensitive group to radiation in STZ molecule due to its high electrophilic feature. Therefore, radicals with unpaired electrons localised on SO<sub>2</sub> group is expected to be produced upon irradiation of STZ as in the case of sulphur-containing compounds (Samoilovich and Tsinober, 1970; Bershov et al., 1975; Huzimura, 1979; Katzenberger et al., 1989; Barbas et al., 1992; Kai and Miki, 1992; Walther et al., 1992). These radicals exhibit no hyperfine structure and they have *g* tensor of orthorhombic symmetry with an average value varying between 2.0037 and 2.0059 (Samoilovich and Tsinober, 1970; Bershov et al., 1975; Huzimura, 1979). Experimental *g* values determined in the present work for intense resonance peaks of the gamma irradiated STZ fall into this range. Consequently, we believe that SO<sub>2</sub><sup>-</sup> ionic (hereafter radical A) and RSO<sub>2</sub><sup>0\*</sup> neutral (hereafter radical B) species are the responsible magnetic units from the three intense resonance peaks appeared at the middle of the ESR spectra of gamma irradiated STZ. Radicals A and

B produced in irradiated crystalline powder of STZ are randomly oriented. However, the motion of species B is restricted, in large extent, due to the big R group attached to it, so that it gives rise to powder spectra with principal *g* values varying between  $g_{xx} = 2.0022$ – $2.0031$ ,  $g_{yy} = 2.0015$ – $2.0098$  and  $g_{zz} = 2.0058$ – $2.0066$  (Bershov et al., 1975; Huzimura, 1979). As for SO<sub>2</sub><sup>-</sup> ionic species, its motional freedom is high due to relatively weak steric effect experienced by this species and, as a result of this, it gives rise to a single resonance line of average spectroscopic *g* factor varying between 2.0037 and 2.0059 (Samoilovich and Tsinober, 1970; Huzimura, 1979). Other plausible species are likely to be produced after hemolytic ruptures of S–N and C–S chemical bonds in irradiated STZ. They are assigned as C and D species, respectively in the present work. However, all species produced after irradiation are expected to undergo immediate germination termination reactions (Tilquin, 1985) due to cage effect. Therefore, the amounts of the species responsible from the ESR spectra would be different depending on the capacity of these species participating to the germination reaction.



Table 4

Decay constants at five different temperatures for the radicals contributing to the ESR spectra of STZ samples irradiated at a dose of 50 kGy

Annealing temperature (K)	Radical species	Decay constants $k \times 10^5 \text{ (min)}^{-1}$	Correlation coefficient ( $r^2$ )
310	A	9 ( $\pm 1$ )	0.96
	B	52 ( $\pm 7$ )	
	C	10660 ( $\pm 325$ )	
	D	2451 ( $\pm 95$ )	
348	A	59 ( $\pm 8$ )	0.97
	B	380 ( $\pm 30$ )	
	C	27000 ( $\pm 430$ )	
	D	11000 ( $\pm 360$ )	
365	A	344 ( $\pm 45$ )	0.98
	B	1230 ( $\pm 75$ )	
	C	46000 ( $\pm 550$ )	
	D	17000 ( $\pm 280$ )	
393	A	1575 ( $\pm 105$ )	0.99
	B	5500 ( $\pm 120$ )	
	C	68000 ( $\pm 310$ )	
	D	35200 ( $\pm 180$ )	
413	A	1675 ( $\pm 120$ )	0.99
	B	6462 ( $\pm 110$ )	
	C	102000 ( $\pm 220$ )	
	D	56207 ( $\pm 205$ )	

Figures in parenthesis indicate the estimated error on the relevant parameters.

Simulation calculations were performed to support the idea put forward and to determine correct spectroscopic parameters of the contributing radical species assuming the presence of four radical species proposed above, exhibiting isotropic (species A, C and D) and axially symmetric (species B)  $g$  tensors. Room temperature experimental signal intensity data obtained for a sample irradiated at a dose of 50 kGy were used as

Table 5

Activation energies calculated from the decay constants derived for samples irradiated at a dose of 50 kGy

Radical species	Activation energy (kcal/mol)	Correlation coefficient ( $r^2$ )
A	14.0 ( $\pm 1.5$ )	0.98
B	12.6 ( $\pm 0.9$ )	0.99
C	5.5 ( $\pm 0.2$ )	0.99
D	7.7 ( $\pm 0.2$ )	0.99

Figures in parenthesis indicate the estimated error on the relevant energy.

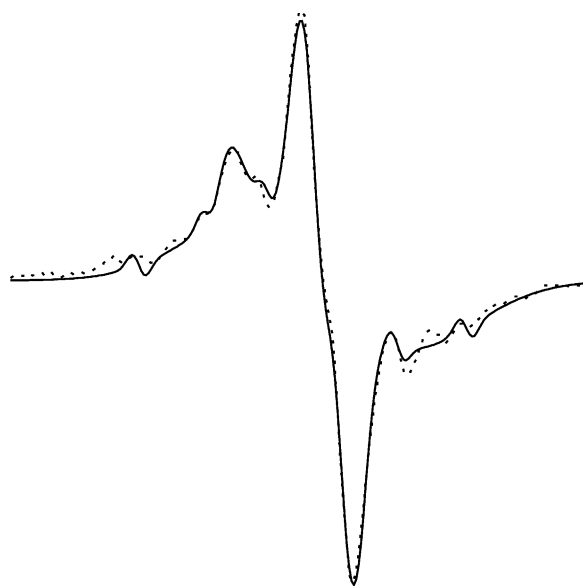


Fig. 6. Experimental and calculated ESR spectra for STZ irradiated at a dose of 50 kGy. Solid line: theoretical; dashed line: experimental.

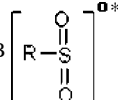
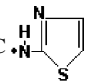
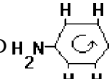
input to carry out the simulation calculations. The results of these calculations are summarized in Table 6, and theoretical spectrum derived using the parameter values given in this table are presented in Fig. 6 with its experimental counterpart. As seen from Table 6, linewidth and relative weight of the radical D are fairly large compared with other species due to unresolved hyperfine splitting originating from equivalent proton of benzen ring and possibly large steric effect experienced by this species. Species B, which has a line width of 1.4 G and relative weight of 0.21, practically dominates ESR spectra due to the distribution of its  $g$  value over a large scale. The agreement between experimental and theoretical spectra derived using calculated parameters is rather good which indicates that the model based on four proposed tentative species of different characteristic features explains well the experimental ESR spectra of irradiated STZ.

### 3.7. FT-IR spectra of STZ

IR spectroscopy was thought to be a complementary technique to elucidate the types and structures of the possible radiation-induced species silent to ESR spectroscopy and, as a result, FT-IR spectra of both



Table 6  
Calculated spectroscopic parameters for proposed radical species

Radical species	g factor	Spectroscopic parameters			Relative weight
		Line width (G)	Hyperfine AN(G)	Splitting AH(G)	
A $\text{SO}_2^-$	$2.0051 \pm 0.0002$	$1.5 \pm 0.2$	–	–	0.06
B 	$2.0106 \pm 0.0002$ $2.0030 \pm 0.0002$	$1.4 \pm 0.2$	–	–	0.21
C 	$2.0059 \pm 0.0002$	$0.8 \pm 0.2$	$13.7 \pm 0.2$	$3.6 \pm 0.2$	0.01
D 	$2.0039 \pm 0.0002$	$8.0 \pm 0.2$	–	$3.2 \pm 0.2$	0.73

unirradiated and 50 kGy gamma irradiated STZ samples were also recorded at room temperature. However, no significant changes in the IR bands of STZ molecule attributable to any final products created by gamma radiation were detected. Therefore, it was concluded that the amounts of the radiation-induced final products were very small not creating any detectable changes in the IR bands originating from undamaged molecules. This result was considered as correlating with relatively small  $G$  value of 0.1 reported in the present work for gamma irradiated STZ by ESR technique. As is known,  $G$  value represents the number of radicals produced by the absorbed radiation per 100 eV (Ikeya, 1993).

#### 4. Conclusions

Although unirradiated STZ exhibits no ESR signal, samples irradiated at room temperature exhibited a complex ESR spectra consisting of 10 resonance peaks, which saturated as inhomogeneously broadened resonance lines in the microwave power range 1–80 mW.

Dose–response curves related with the studied resonance peaks follow exponential increases in the radiation dose range of 5–50 kGy.

Radical species responsible from experimental ESR spectra are unstable at normal (290 K open to air) and stability (313 K and 75% relative humidity) conditions, and they decay nearly completely over a period of 50 days at normal conditions and still faster at stability

conditions. A model based on four tentative radical species, decaying with different rates, was found to explain well experimental decay data obtained for studied resonance peaks.

Although radical species undergo reversible changes below room temperature, they show irreversible change above 320 K.

Annealing samples at high temperatures produce much faster decay in the peak heights due to significant decrease in cage effects, which causes an increase in the radical encounter frequency giving rise to fast decay of the radical species at these temperatures. However, decay activation energies of the radical species are not same. Although activation energies of species C and D are almost similar ( $5.5 \pm 0.2$  and  $7.7 \pm 0.2$  kcal/mol, respectively), they are much smaller than those obtained for species A ( $14.0 \pm 1.5$  kcal/mol) and B ( $12.6 \pm 0.9$  kcal/mol).

A model based on four tentative species having different features was found to explain well ESR data obtained for STZ gamma irradiated up to 50 kGy. Species B dominates the shape of experimental ESR spectra due to its narrow linewidth although it has a weight smaller than that obtained for species D.

Radiation yield of STZ is calculated to be fairly small ( $G = 0.1$ ) compared with those reported for sulfonamide solutions ( $G$  varies in the range of 3.5–5.1), but it falls into the range of the  $G$  values reported for solid sulfonamides (0.15–0.6) (Philips et al., 1971, 1973). This difference in  $G$  values was believed to originate from hydrated electron ( $e_{\text{aq}}^-$ ) and hydroxyl radicals

(•OH) produced in large amount as radiolytic intermediates in irradiated aqueous solutions of sulfonamides. Although, the sensitivity of STZ to gamma radiation is not high, the detection and discrimination of unirradiated STZ from irradiated one turns out to be possible even at low radiation doses (Fig. 2a).

Gamma radiation dose up to 50 kGy creates no changes in the amount of STZ molecules detectable by FT-IR spectroscopy.

Basing on the above results, it was concluded that gamma radiation doses up to 50 kGy produce relatively low-amount radicalic intermediates in irradiated STZ and that ESR spectroscopy can be used as a potential technique to characterize these intermediates.

## Acknowledgments

We thank Professor Dr. Yekta Özer from Faculty of Pharmacy of Hacettepe University for providing kindly STZ samples of spectroscopic grade.

## References

- Barbarin, N., Rollmann, B., Tilquin, B., 1999. Role of residual solvents in the formation of volatile compounds after radiosterilization of cefotaxime. *Int. J. Pharm.* 178, 203–212.
- Barbas, M., Bach, A., Mudelsee, R., Mangini, A., 1992. General properties of the paramagnetic center at  $g = 2.006$  in carbonates. *Quat. Sci. Rev.* 11, 165–171.
- Basly, J.P., Duroux, J.L., Bernard, M., 1996. Gamma radiation induced effects on metronidazole. *Int. J. Pharm.* 139, 219–221.
- Basly, J.P., Basly, I., Bernard, M., 1999. Radiation induced effects on cephalosporins: an ESR study. *Int. J. Radiat. Biol.* 75, 259–263.
- Bershov, L.V., Martirsyan, V.O., Marfunin, A.S., Speranskii, A.V., 1975. EPR and structure models for radical ions in anhydrite crystals. *Fortschr. Mineral.* 52, 591–604.
- Bhalla, H.L., Menon, M.R., Gopal, N.G.S., 1983. Radiation sterilization of polyethylene glycols. *Int. J. Pharm.* 17, 351–355.
- Boess, C., Bögl, K.W., 1996. Influence of radiation treatment on pharmaceuticals. A review: alkaloids, morphine derivatives, and antibiotics. *Drug Dev. Ind. Pharm.* 22, 495–529.
- Bögl, K.W., 1989. Identification of irradiated foods-methods, development and concepts. *Appl. Radiat. Isot.* 40, 1203–1210.
- Ciranni Signoretti, E., Onori, S., Valvo, L., Fattibene, P., Savella, A.L., De Sena, C., Alimonti, S., 1993. Ionizing radiation induced effects on cephradine, influence of sample moisture content, irradiation dose and storage conditions. *Drug Dev. Ind. Pharm.* 19, 1693–1708.
- Ciranni Signoretti, E., Valvo, L., Fattibene, P., Onori, S., Pantoloni, M., 1994. Gamma radiation-induced effects on cefuroxime and cefotaxime. Investigation on degradation and syn-anti isomerization. *Drug Dev. Ind. Pharm.* 20, 2493–2508.
- Clarke's Isolation Identification of Drugs in Pharmaceuticals, Body Fluids and Post-Mortem Material, 1986. In: Moffot, A.C., Jackson, J.V., Moss, M.S., Widdop, B. (Eds.), 2nd ed., The Pharmaceutical Press, London, pp. 978–995.
- Delincée, H., 1991. Analytical Methods For Irradiated Foods: A Review of Current Literature. IAEA-TECDOC-587. International Atomic Agency, Vienna.
- Desrosiers, M.F., Wilson, G.L., Hutton, D.R., Hunter, C.R., 1991. *Appl. Radiat. Isot.* 42, 613–616.
- Gibella, M., Crucq, A.S., Tilquin, B., Stocker, P., Lesgards, G., Raffi, J., 2000. ESR studies of some irradiated pharmaceuticals. *Radiat. Phys. Chem.* 58, 69–76.
- Gopal, N.G.S., 1978. Radiation sterilization of pharmaceuticals and polymers. *Radiat. Phys. Chem.* 12, 35–50.
- Huzimura, R., 1979. ESR studies of radical ion centers in irradiated  $\text{CaSO}_4$ . *Jpn. J. Appl. Phys.* 18, 2031–2032.
- Ikeya, M., 1993. New applications of electron spin resonance-dating, dosimetry and microscopy. World Scientific Publishing Co. Pte. Ltd.
- Jacobs, G.P., 1995. A review of the effects of gamma radiation on pharmaceutical materials. *J. Biomater. Appl.* 10, 59–96.
- Kai, A., Miki, T., 1992. Electron Spin Resonance of Sulfite Radicals in Irradiated Calcite and Aragonite. *Radiat. Phys. Chem.* 40, 469–476.
- Katzenberger, O., Debuyst, R., De Canniere, P., Dejehet, F., Apers, D., Barabas, M., 1989. Temperature experiments on mollusk samples: an approach to ESR signal identification. *Appl. Radiat. Isot.* 40, 1113–1118.
- Miyazaki, T., Arai, J., Kaneko, K., Yamamoto, K., Gibella, M., Tilquin, B., 1994. Estimation of irradiation dose of radiosterilized antibiotics by ESR: ampicillin. *J. Pharm. Sci.* 83, 1643–1644.
- Onori, S., Pantoloni, M., Fattibene, P., Ciranni Signoretti, E., Valvo, L., Santucci, M., 1996. ESR identification of irradiated antibiotics: Cephalosporins. *Appl. Radiat. Isot.* 47, 1569–1572.
- Philips, G.O., Power, D.M., Sewart, M.C.G., 1971. Effect of gamma irradiation on sodium sulphacetamide. *Radiat. Res.* 46, 236–250.
- Philips, G.O., Power, D.M., Sewart, M.C.G., 1973. Effect of gamma irradiation on sulphonamides. *Radiat. Res.* 53, 204–215.
- Raffi, J.J., Stevenson, M.H., Kent, M., Thiery, J.M., Belliaro, J.J., 1992. *Int. J. Food Sci. Technol.* 27, 111–124.
- Raffi, J., Delincée, H., Marchioni, E., Hasselmann, C., Sjöberg, A.M., Leonardi, M., Kent, M., Bögl, K.W., Schreiber, G., Stevenson, H., Meier, W., 1994. Final Report on New Methods for the Detection of Irradiated Food, BCR, CEC, Luxembourg, EUR 15 261 EN.
- Raffi, J., 1998. Identifying Irradiated Foods. *Trends Anal. Chem.* 17, 226–233.
- Reid, B.D., 1995. Gamma processing technology. An alternative technology for terminal sterilization of parenterals. *J. Pharm. Sci. Technol.* 49, 2.
- Samoilovich, M.I., Tsinober, L.I., 1970. Characteristics of radiation color centers and microisomorphism in crystals. *Sov. Phys. Crystallogr.* 14, 656–666.

- Schuler, R.H., 1994. Three decades of spectroscopic studies of radiation produced intermediates. *Radiat. Phys. Chem.* 43, 417–423.
- Stark, P.A., 1970. *Introduction to Numerical Methods*. Macmillan Publishing Co. Inc, London, p. 273.
- The Merck Index, 1989. In: Budavari, S., O'Neil, M.J., Smith, A., Heckelman, P.E. (Eds.), *An Encyclopedia of Chemicals, Drugs and Biologicals*, 11th ed., Merck and Co. Inc, USA, pp. 1403–1412.
- Tilquin, B., 1985. *Composant Radicalaire des Transformations Radio-initiées Dans Les Alcanes à 77 K* Thèse Dagrégation. UCL, Ciaco-la-Neuve, Belgique.
- Walther, R., Barbas, M., Mangini, A., 1992. Basic ESR studies on recent corals. *Q. Sci. Rev.* 11, 191–196.